Linear Viscoelastic Diffusion in the Poly(styrene)/Ethylbenzene System: Differential Sorption Experiments

G. F. Billovits and C. J. Durning*

Department of Chemical Engineering, Materials Science and Mining, Columbia University, New York, New York 10027

Received May 26, 1993; Revised Manuscript Received September 7, 1993®

ABSTRACT: Mutual diffusion was studied in the poly(styrene) (PS)/ethylbenzene system using differential vapor sorption. A series of differential sorptions was carried out at 40 °C on a thin film ($\simeq$5 μm) of nearly monodisperse PS ($M_n \simeq 305\,000$; $M_w/M_n \simeq 1.05$). The smallest possible increments in ethylbenzene pressure were used so that very small changes in composition were realized during each sorption. Consequently, the experiments closely approximate a linear perturbation limit. Viscoelastic (non-Fickian) diffusion was observed over the range of ethylbenzene weight fractions $0.03 < \omega_1 < 0.12$. A characteristic sequence of viscoelastic weight uptake curves was found with increasing ω_1 in this range; the sequence resembles that found by Odani and co-workers[8–11] many years ago. A calculation of diffusion Deborah numbers suggests that relaxation mechanisms associated with both the transition and terminal regions of the linear viscoelastic spectrum play a role in the diffusion process.

Introduction

Mutual diffusion erases concentration gradients in a binary fluid mixture. For mixtures of simple, viscous fluids, Fick' law can adequately describe the process in the continuum limit. However, when one component is polymeric, Fick's equation often fails.[1,2] In such cases the diffusion is called non-Fickian or viscoelastic. A good understanding of viscoelastic diffusion is important in polymer material processing since it is a controlling physical process in many processing operations, including devolatilization, fiber-spinning, coating and drying operations, and microlithography.

Durning and Tabor[3] developed a thermodynamic theory for the limiting case of linear viscoelastic diffusion, i.e. for viscoelastic diffusion with infinitesimal changes in composition. It qualitatively reproduces many of the non-Fickian features observed[3–6] but quantitative tests of the theory, or of any similar theory (e.g. Lustig et al.[7]), have been hampered by a lack of reliable data in the linear limit. The most systematic study focusing on this limit was published by Odani and co-workers[8–11] more than 25 years ago; unfortunately, they employed rather poorly characterized polymer samples, making quantitative comparisons with theory difficult.[4,5] In addition, the auxiliary data necessary for parameter estimations in the theory (linear viscoelastic mechanical data) have not been measured at the relevant temperatures and compositions in any of the systems they studied.

In this work, we report new linear viscoelastic diffusion experiments in the poly(styrene)/ethylbenzene system. We constructed a quartz-spring vapor sorption balance for this purpose and carried out a series of differential sorptions in a well-characterized, thin polystyrene film under the smallest possible driving forces. The data enable a critical test of continuum-level theories since adequate auxiliary mechanical data have been published recently for this system;[12] a detailed comparison between theory and experiment will appear in a subsequent article.

Background

Differential Sorption Technique. A number of techniques have been applied to study viscoelastic diffusion. Among these are sorption/desorption,[13] dynamic light scattering,[14] ion back-scattering,[15] and interferometry.[16] The methods differ in the accessible range of length scale, composition, and temperature. We focus on sorption in this work, since the method permits clear observation of distinctive viscoelastic effects over a range of conditions typical in applications. Further, the interpretation of sorption data is unambiguous.

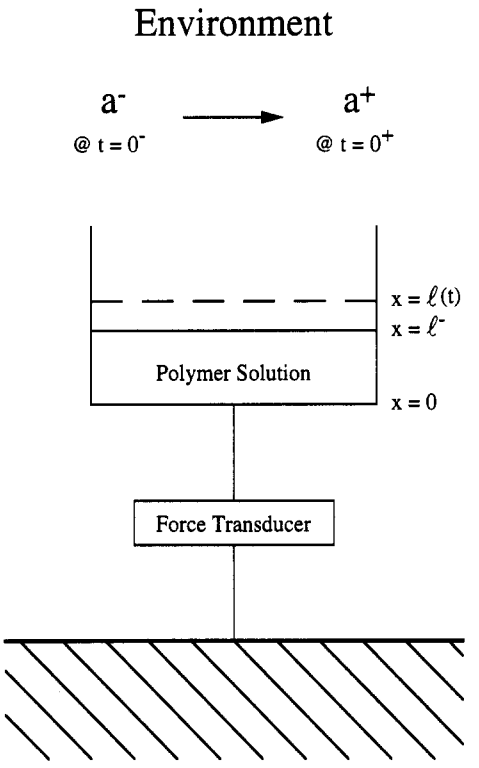

Figure 1. Schematic of one-dimensional sorption experiment.

Figure 1 shows a schematic of a one-dimensional sorption experiment: A thin supported film of the mixture resides in an infinite reservoir of the fluid's vapor at a controlled activity. By symmetry, this is exactly the situation for an unsupported film exposed to vapor on both sides. Initially, the mixture contains a fluid weight fraction ω_1^-, dictated by equilibrium with the reservoir at a fluid activity a^-. At time $t = 0$ the activity in the reservoir is increased to a^+, and fluid diffuses into the condensed mixture, causing an increase in its mass. A new equilibrium is eventually

* To whom correspondences should be sent.
® Abstract published in *Advance ACS Abstracts*, October 15, 1993.

0024-9297/93/2226-6927$04.00/0

established with a fluid weight fraction ω_1^+. If $a^- = 0$ and $a^+ \sim O(1)$, then the experiment is termed an *integral sorption*. However if $a^- \neq 0$ and a^+ only slightly exceeds a^-, the experiment is termed a *differential* or *interval sorption*. In either case the kinetics of diffusion are tracked by weighing the film to determine the mass uptake of fluid as a function of time.

For an integral sorption, a relatively large increase in the fluid content typically occurs, causing the transport properties to vary significantly with time and position; consequently, the diffusion is usually nonlinear during an integral sorption. For differential sorption, the composition change can be made very small (i.e. $\omega_1^+ - \omega_1^- \ll 1$) so that the local transport properties remain essentially constant. In this case the diffusion is linear (i.e. a mathematical model for the composition field is a linear initial value problem). Our investigation focuses on the linear limit.

Previous Experimental Work. Odani and co-workers[8-11] carried out differential sorptions in several amorphous polymer/organic fluid systems. Plots of fluid mass uptake (M_t) versus the square root of time ($\sqrt{t}$) for successive differential sorptions with increasing mean fluid content followed a characteristic sequence:

$$\text{sigmoid} \rightarrow \text{pseudo - Fickian} \rightarrow \text{two-stage} \rightarrow \text{pseudo - Fickian} \rightarrow \text{Fickian} \quad (1)$$

For the first few intervals, where the fluid weight fraction is very low and the glass transition temperature (T_g) of the mixture lies well above the experimental temperature, "sigmoid" or S-shaped fluid weight uptake curves were found. For intervals at somewhat higher fluid concentrations, the behavior resembled the predictions from Fick's law (the initial fluid weight uptake increased linearly with $\sqrt{t}$); however, the final approach to equilibrium was protracted, so that behavior was termed "pseudo-Fickian". At still higher fluid concentrations, "two-stage" sorption was observed, where M_t appears to reach an equilibrium level rather quickly but subsequently relaxes upward to the true equilibrium value over a long time scale. As the mean fluid content was increased further, another region of pseudo-Fickian plots was typically encountered, and finally, for intervals at the highest fluid concentrations possible in the equipment, where T_g for the mixture lies well below the experimental temperature, Fickian behavior was observed. It should be emphasized that none of the behaviors observed in the sequence (1), except of course the final Fickian curves, can be explained by Fick's laws.

Several deviations from sequence (1) have been reported and are worth noting. Odani and co-workers[9,10] also studied several semicrystalline polymers. Instead of the sequence (1), they found

$$\text{sigmoid} \rightarrow \text{pseudo - Fickian} \rightarrow \text{two-stage} \rightarrow \text{sigmoid}$$

Berens and Hopfenberg[17] carried out differential sorptions of organic vapors in microspheres of polystyrene (PS) and poly(vinyl chloride) (PVC) prepared by emulsion polymerization. For *n*-hexane sorption in PS at 30–40 °C, and for acetone, methanol, and vinyl chloride monomer sorption into PVC at 30–40 °C, runs at the lowest fluid concentrations showed Fickian rather than sigmoid shaped uptake curves. At higher fluid contents, the behaviors observed conform to the remainder of the sequence (1) except for a "sorption overshoot" during the uptake of methanol in PVC at intermediate concentrations: The weight uptake passed through a conspicuous relative maximum before ascending to the final, higher equilibrium level. Vrentas et al.[18] reported a somewhat different type of overshoot during the differential sorption of ethylbenzene in poly(ethyl methacrylate) at relatively high fluid weight fractions, well above T_g. They found uptakes which rose to an absolute maximum before slowly decreasing to the final equilibrium value. The significance and origin of sorption overshoots is equivocal since the reported observations do not fit into a consistent pattern.

Another relevant study worth mentioning used a different type of linear sorption experiment called "oscillatory sorption". With oscillatory sorption, one applies a small amplitude sinusoidal variation of the activity in the reservoir, instead of the small amplitude step used in differential sorption. Vrentas et al.[19] studied poly(vinyl acetate)/water at 90 °C and poly(vinyl acetate)/methanol at 60 °C by this method. In a series of experiments, at a constant temperature and mean fluid composition, in which the frequency of the external fluid activity was varied, they found in both systems regions of Fickian response at low and high frequencies separated by a region of linear viscoelastic diffusion at intermediate frequencies.

Deborah Number Correlation

Elastic, Viscous, and Viscoelastic Diffusion. Vrentas and Duda[20,21] suggested a method of predicting the conditions for linear viscoelastic diffusion based on the value of a diffusion Deborah number, $(DEB)_D$:

$$(DEB)_D = \tau/\theta_D \quad (2)$$

where τ is a characteristic relaxation time of the mixture and θ_D is a characteristic time for the mutual diffusion process. Using their procedure (see below) one can assign a unique value of $(DEB)_D$ to any linear diffusion experiment and, presumably, anticipate whether viscoelastic effects will appear on the basis of its value.

If $(DEB)_D \gg 1$, then the time scale for dominant molecular relaxations greatly exceeds the diffusion time and there is, effectively, no reconfiguration of macromolecules during the process. Here, mutual diffusion resembles fluid diffusion in an elastic medium; Vrentas and Duda termed this case "elastic" and anticipated that Fick's theory should govern. (For example, if disentanglement is the dominant relaxation process in response to a small amplitude osmotic field, then mutual diffusion should resemble collective diffusion in an elastic gel when $(DEB)_D \gg 1$, which obeys Fick's laws.)

If $(DEB)_D \ll 1$, molecular relaxation processes occur much more quickly than mutual diffusion. In effect, the polymer component is instantaneously relaxed and behaves like an ordinary viscous fluid and, therefore, the classical Fickian theory should again govern. This case was termed "viscous" diffusion. If $(DEB) \sim O(1)$, molecular relaxation and mutual diffusion have comparable time scales and one anticipates that the relaxation processes may affect the dynamics. Vrentas and Duda suggested that viscoelastic or non-Fickian diffusion, such as reported by Odani et al., should appear in this case.

Calculation of $(DEB)_D$ in Polymer Solutions. Vrentas and Duda[21] proposed a method for calculating $(DEB)_D$ using a modicum of mutual diffusion data in the viscous regime ($(DEB)_D \ll 1$), linear viscoelastic mechanical data, and the free volume theory. The characteristic diffusion time was taken as

$$\theta_D = \frac{L^2}{D^*} \quad (3)$$

where L is the diffusion path length (e.g. the film half-thickness for differential sorption) and

$$D^* = x_1 D_2 + x_2 D_1 \quad (4)$$

where x_1 and x_2 are the mole fractions of the fluid and polymer, respectively, and D_1 and D_2 are the corresponding

self-diffusion coefficients. (D^* is on the order of the binary mutual diffusion coefficient.)

They suggested the terminal time for τ:

$$\tau = \frac{\int_0^\infty sG(s)\,ds}{\int_0^\infty G(s)\,ds} = \eta_0 J_e^0 \qquad (5)$$

where $G(t)$ is the shear relaxation modulus at the conditions of interest, η_0 is the zero-shear viscosity, and J_e^0 is the steady-shear compliance. (This definition implies that disentanglement is the only relevant molecular relaxation process.) In order to evaluate $(DEB)_D$ at conditions of interest, τ must be known as a function of temperature (T), fluid mass fraction (ω_1), and polymer molecular weight (M_2). Vrentas and Duda suggested that a measured reference value of τ, τ_o, be corrected by a shift factor, a_{TC}:

$$\tau(T,\omega_1,M_2) = a_{TC}(T,T_o,\omega_1,\omega_{1o},M_2,M_{2o})\tau_o(T_o,\omega_{1o},M_{2o})$$

where the subscript o indicates reference conditions. Neglecting the dependencies of J_e^0 on T and ω_1 and using Bueche's[24] semiempirical relationship between η_0 and the polymer self-diffusion coefficient D_2, they derived

$$(DEB)_D = \frac{D_{2o}(T_o,\omega_{1o},M_{2o})\tau_o(T_o,\omega_{1o},M_{2o})}{L^2}\left(\frac{D_1(T,\omega_1,M_2)}{x_2 D_2(T,\omega_1,M_2)} + x_1\right) \qquad (6)$$

as a useful expression for calculating $(DEB)_D$. Application of eq 6 requires reference values of τ and D_2 as well as a method for evaluation of the ratio D_1/D_2 over a broad range of conditions. The last can be accomplished using the free volume theory.[22,23]

Prior Applications of the $(DEB)_D$ Correlation. Using the above method, Vrentas et al. calculated $(DEB)_D$ over a range of temperatures for the poly(styrene) (PS)/*n*-pentane system[20] in the limit $\omega_1 \to 0$, and for the systems PS/ethylbenzene[21] and poly(ethyl methacrylate)/ethylbenzene[18] over the complete range of ω_1 for a broad range of temperatures. Durning and co-workers calculated $(DEB)_D$ by a somewhat different method for the systems poly(methylmethacrylate)/methyl acetate[4] and poly(vinyl acetate)/water.[3] In the last three cases, the predictions for the appearance of viscoelastic diffusion in differential sorption experiments based on $(DEB)_D$ were compared with experiment and were largely confirmed.

An unexplained exception to the correlation should be noted, however. Vrentas and Duda argued that for $(DEB)_D \gg 1$ Fick's laws should govern; this has been verified in some investigations,[17] but in all of the amorphous polymer/fluid systems studied by Odani et al.,[8-11] sigmoid uptake curves were observed in the elastic limit (i.e. $(DEB)_D \gg 1$ which holds at very low fluid weight fractions, well below T_g). Vrentas and Duda[21] explained this inconsistency by suggesting that a time dependent surface concentration plays a role during sorption at these conditions. However, they offered no clue for the molecular origin of such a drift in surface concentration, nor did they address the conceptual inconsistency in having a retarded surface response under conditions where an elastic (instantaneous) response is expected.

Predictions for the Poly(styrene)/Ethylbenzene System. Vrentas and Duda's calculation of $(DEB)_D$ for the poly(styrene)/ethylbenzene system (Figure 5 of ref 21) is reproduced in Figure 2, which shows the T–ω_1 map with isoclines of $(DEB)_D$ for $L = 10^{-3}$ cm and $M_2 = 3 \times 10^5$. Regions of linear elastic (Fickian), linear viscous (Fickian), and linear viscoelastic (non-Fickian) diffusion are indicated.

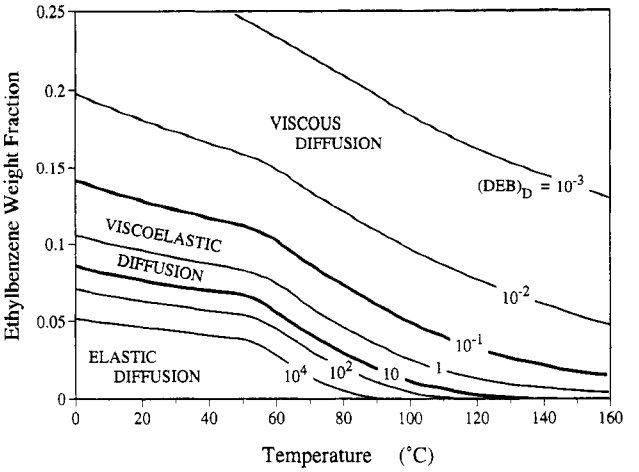

Figure 2. $(DEB)_D$ map for the poly(styrene)/ethylbenzene system with $M_2 = 3 \times 10^5$ and $L = 10^{-3}$ cm. The map corresponds to Figure 5 in ref 21.

For a series of differential sorptions at 40 °C starting from $\omega_1 = 0$, the calculation predicts that the first few weight uptake curves should exhibit the Fickian response since $(DEB)_D \gg 1$. At $\omega_1 \simeq 0.07$ viscoelastic features ought to emerge (e.g. sigmoid, pseudo-Fickian, and two-stage weight uptake curves). Viscoelastic effects should persist until $\omega_1 \simeq 0.12$, when the behavior should again revert to classical Fickian. In what follows we describe our experimental findings for precisely this series of differential sorptions.

Experimental Section

Quartz-Spring Vapor Sorption Balance. For the differential sorption experiment shown schematically in Figure 1, a sensitive force transducer allows one to measure the mass of the solution as a function of time after incrementing the fluid activity in the environment. We employed a helical fused-quartz spring (Worden Quartz, Houston TX) with a (nominal) capacity of 200 mg and a maximum extension of 350 mm from the zero-load state. The manufacturer specified the spring as linear to within 2% over the entire range of extension. A quartz-spring was chosen over an electromechanical transducer because exposure to organic vapors, which can destroy electromechanical units, has no effect on the spring's performance.

A spring-balance apparatus similar to those described by Fujita and Kishimoto[25] and Prager and Long[26] was designed and constructed. A polymer film sample is suspended within one of two jacketed spring cases, resting on a massive marble slab isolated from the lab bench by shock mounts. The cases are connected to a one-piece borosilicate glass vacuum manifold by flexible steel bellows which eliminate vibrations through the manifold. Temperature control inside the spring cases is ensured by circulating water through jackets surrounding the cases from a thermostatically controlled bath. The manifold includes a 5-L buffer volume which provides an effectively infinite vapor reservoir during sorption. The pressure within the manifold is monitored by a mercury manometer. These components are enclosed in a well-mixed, thermostatically controlled air bath. Extension of the springs is measured with a specially constructed cathetometer (sensitivity ± 1 μm) mounted on the marble slab. Also connected to the vacuum manifold, but located outside the air bath, are a liquid reservoir bulb which provides the vapor source, a thermocouple gauge for measuring the vacuum during the initial system evacuation, and the vacuum pumps, equipped with liquid nitrogen traps.

Throughout the apparatus, greaseless, high vacuum valves with Teflon plungers and Viton O-rings are employed. Stainless steel bellows with high vacuum glass–metal joints have also been used between the manifold and vacuum pumps in order to dampen vibrations from the pumps. The manifold is serviced by a two-

stage rotary vacuum pump (Sargent Welch Model 1402) and a triple-stage, water-cooled mercury diffusion pump (Eck & Krebs, Model 4050) capable of an ultimate vacuum of 10^{-7} Torr. Constant temperature in both the air and water baths is maintained by a pair of temperature controllers (Yellow Springs Instruments Model 63RC, nominal accuracy ±0.05 °C).

Procedures. Operation of the balance begins with thorough degassing of the liquid in the reservoir bulb by repeated freeze–thaw cycles. Then, after loading a film sample into a spring case, the entire apparatus is thoroughly evacuated to remove all gases and volatile materials. This process requires at least 1 week of continuous pumping at high vacuum (using the diffusion pump) to remove substances, such as water, which tend to adsorb strongly on the walls of the apparatus. This evacuation was carried out at the temperature of the sorption experiments.

After evacuation, a series of differential sorption experiments was intitiated by closing a valve to isolate the spring case from the manifold. Vapor was then admitted to the manifold by carefully opening the liquid reservoir until the desired small increase in pressure was achieved. The section of manifold contained in the air bath was then isolated. After allowing the system to reach thermal equilibrium (several hours), the first differential sorption run was begun by opening the spring case to the manifold and tracking the extension of the spring with the cathetometer until equilibrium was established. The spring extension, Δz, was measured from the position of a characteristic point at the end of the spring relative to the end of a reference fiber hung from the same point as the spring.

In order to determine the absolute sample mass the dry, wire-mounted film was weighed immediately prior to loading in the spring case. The apparent increase in weight from the initial dry value due to absorption of vapor into the film can then be determined from Δz using the spring constant calculated from a calibration. The calibration was prepared by plotting Δz versus weight for a series of known weights hung from the spring in vacuum at 35 °C. The calibration verified the spring's linearity and gave the spring constant of 1.801 ± 0.006 mm/mg.

The apparent sample mass measured during a sorption experiment, determined from Δz, was corrected by buoyancy. This correction normally requires that one know the volume of the sample, which was not measured directly. Instead, we measured Δz for the dry sample as a function of pressure in anhydrous air, which does not sorb appreciably into the polymer. A plot of Δz versus pressure, p, was found to be linear; its slope, together with the assumptions that both air and ethylbenzene vapor behave as ideal gases under the conditions of our experiments, gave the buoyancy correction for ethylbenzene:

$$\left(\frac{\Delta z}{p}\right)_{eb} = \frac{M_{eb}}{M_{air}}\left(\frac{\Delta z}{p}\right)_{air} = (1.1 \pm 0.4) \times 10^{-3} \text{ mm/Torr}$$

where M_{eb} and M_{air} mean the molecular weights of ethylbenzene and air, respectively. This value was used to correct all of the sorption data described subsequently for buoyancy.

Materials. ACS reagent grade ethylbenzene, obtained from Aldrich Chemical (Milwaukee, WI) was used as received. The polymer was a 305 000 molecular weight ($\bar{M}_n$) poly(styrene) (PS) with a low polydispersity ($\bar{M}_w/\bar{M}_n < 1.05$) obtained from Polymer Laboratories Ltd. (Church Stretton, UK).

Thin PS films were prepared by spin casting 15–20 weight % solutions of polymer in toluene (ACS reagent grade, Fisher Scientific, Fair Lawn NJ) onto a $3^1/_4$-in. (8.255-cm) diameter silicon wafer using a photoresist spinner (Headway Research, Garland TX); the spinning conditions were 3000 rpm for 30 s. After the supported film was dried in air at room temperature for about 6 h, the film was delaminated from the wafer by leaching in methanol at room temperature for several hours. To handle the ~5 μm thick films prepared by this procedure, each was adhered to a fine wire hoop using small amounts of the casting solution as an adhesive. To minimize absorption of water vapor, the wire mounted films were stored in a desiccator over $CaCl_2$ until used. Before loading into the spring case, each film sample was annealed in vacuo (~0.1 Torr) at 80 °C for 24 h and slowly cooled to room temperature. It was necessary to eliminate static charges on the films by bringing each into close proximity with a Polonium 210α particle source for several minutes just prior to loading.

Results and Discussion

General Features. A series of differential sorptions was carried out at 40 °C. All of the runs reported below were performed on a single, wire-mounted PS film sample. The dry film had a uniform thickness of 5 μm as measured with a dial gauge comparator (Standard, sensitivity ±0.5 μm); its weight was 27.0 ± 0.1 mg.

Eighteen sorption runs were made over a time span of approximately 5 months. The data were collected in five separate "passes", each beginning at a low ethylbenzene pressure and terminating at a higher ethylbenzene pressure after a number of differential sorptions with successive, small increments in pressure. Each pressure increment was kept as small as possible (<2 Torr per interval) in order to keep the concentration interval spanned by each sorption small. The corresponding intervals of ethylbenzene weight fraction, $\Delta\omega_1$, ranged from ~0.006 to ~0.037, which closely approximates the conditions for linear sorption ($\Delta\omega_1 = 0.01$ changes the mutual diffusion coefficient by roughly 10% in this system, as estimated by free volume theory[22,23]). Figure 3 shows the data in each pass (after correcting for buoyancy as discussed above) plotted as weight % ethylbenzene (dry polymer basis) versus $\sqrt{t}$ along with the pressure interval for each run. The highest ethylbenzene content examined was ~17 weight % (run R18) which corresponds to a total spring extension of only ~8 mm over the whole 5-month period. The longest run, R3, required 32 days to reach equilibrium, while for the shortest run, R18, ~85% of the ultimate uptake was achieved within the first minute.

For each sorption run, one can assign a mean ethylbenzene content, $\langle\omega_1\rangle$. Four distinct types of weight uptake plots were found over the range of $\langle\omega_1\rangle$: (1) for a trace of ethylbenzene (<1%), slow, monotonic fluid uptake is observed, which closely resembles the pseudo-Fickian behavior indicated in sequence 1; (2) for ethylbenzene contents in the range $0.01 \leq \langle\omega_1\rangle \leq 0.105$, the weight uptake plots are two-stage; (3) for ethylbenzene contents in the range $0.105 \leq \langle\omega_1\rangle \leq 0.13$, the uptake curves are sigmoid, but show a very slow approach to the final equilibrium value; (4) at ethylbenzene contents $\langle\omega_1\rangle > 0.13$, the sorption process appears to be Fickian.

There were no indications of sorption overshoots observed at any of the conditions studied. In the following sections, we discuss the sorption isotherm, demonstrate the reproducibility of the data, and discuss in more detail the trends with $\langle\omega_1\rangle$ observed in the sorption kinetics. However, a few additional generic remarks are appropriate first.

Making multiple passes has several advantages in differential sorption. One does not, in general, achieve identical values of $\langle\omega_1\rangle$ for runs in successive passes, so multiple passes allow one to examine the effect of $\langle\omega_1\rangle$ in fine detail. If, by coincidence, two runs in successive passes have identical values of $\langle\omega_1\rangle$, one can assess reproducibility of the data; this was done in our study.

Some of the passes in our study were initiated because of an experimental difficulty. Pass 2 was initiated because a circulating fan in the air bath had to be replaced, while pass 3 was undertaken because the experimental time scale was overestimated in run R8, leading to a scarcity of data at short times. In all cases, a new pass was initiated by reducing the ethylbenzene pressure to an appropriate level and waiting until a new equilibrium was established.

Run R2 requires special comment. Here, the ethylbenzene uptake increases gradually to a nearly static value, drops very suddenly, the subsequently increases to roughly

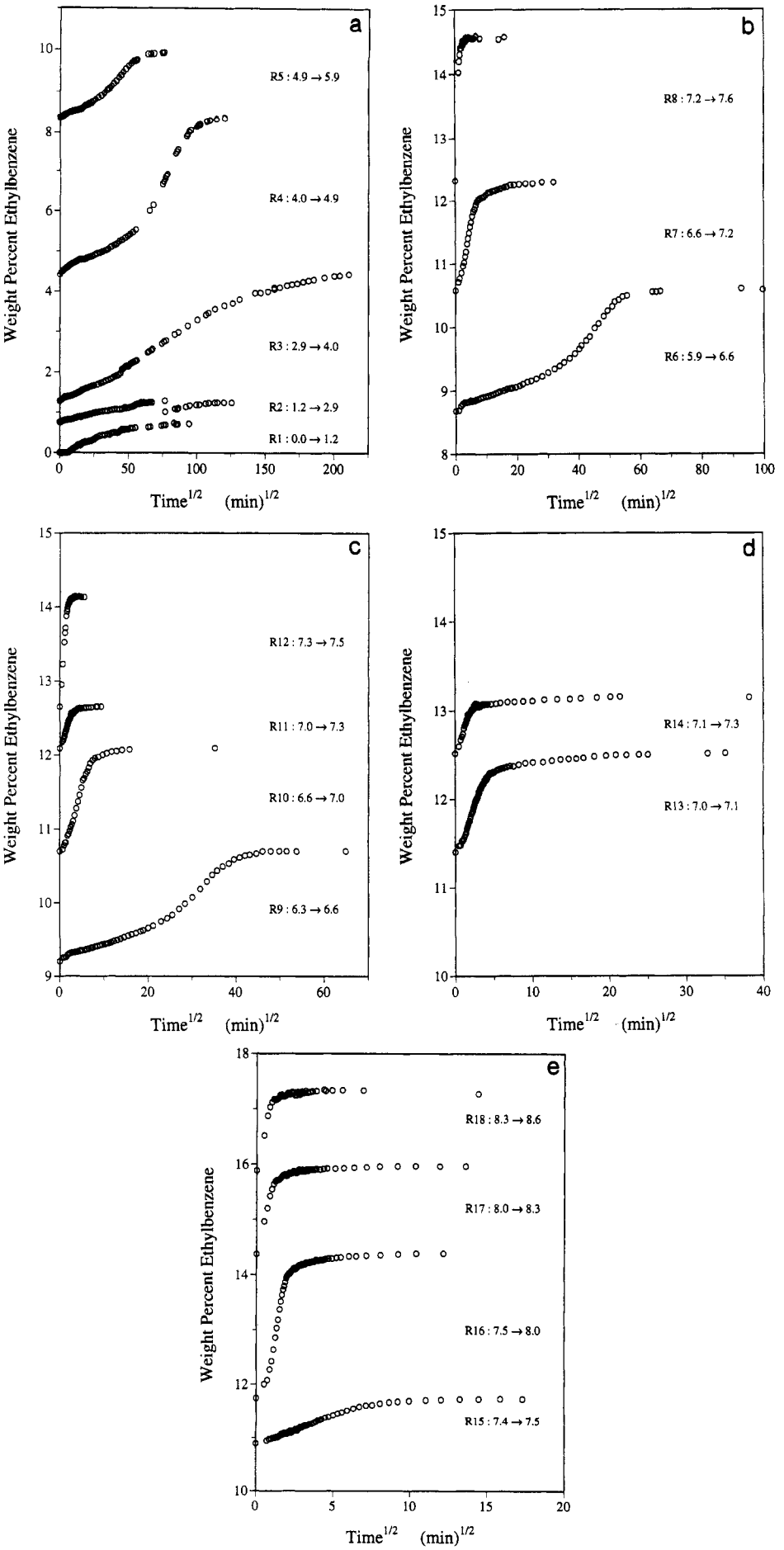

Figure 3. Ethylbenzene weight uptake (% dry polymer) versus $\sqrt{t}$ during (a) pass 1, (b) pass 2, (c) pass 3, (d) pass 4, and (e) pass 5. The pressure interval in Torr is indicated for each run.

the same static point (see Figure 3a). It was noted at ~50 h into the experiment ($\sqrt{t} \simeq 55$ min$^{1/2}$) that the polymer film had made contact with the wall of the spring case. In order to dislodge the sample from the wall, at ~90 h into

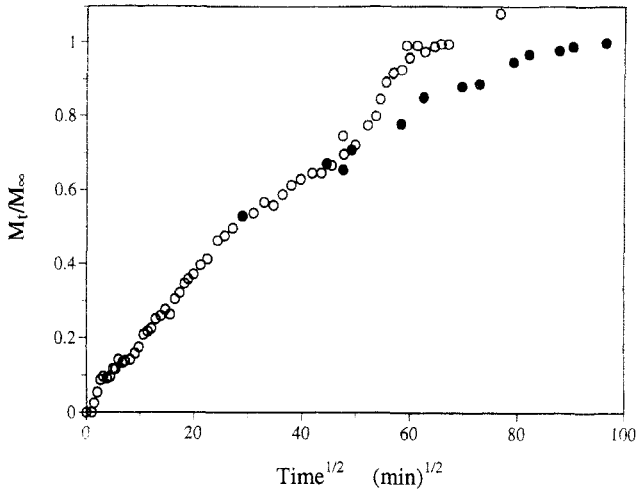

Figure 4. M_t/M_∞ versus $\sqrt{t}$ for run R2 showing the data before opening the air bath (○) and after (●), the latter shifted to coincide with the former.

the experiment ($\sqrt{t} \simeq 77$ min$^{1/2}$) the air bath was opened for about 20 min and the spring case was reoriented to provide ample clearance for the sample. This caused a decrease of the ethylbenzene content, since opening the air bath reduced the temperature, and therefore the ethylbenzene pressure, within the manifold. This evidently led to desorption of ethylbenzene from the film. Figure 4 shows that if the data after opening the air bath are shifted horizontally back to the point where they intersect the data prior to opening the air bath, a smooth, monotonic increase in ethylbenzene content is obtained. This correction is marginal and, therefore, one should not take the data from R2 too seriously. No further difficulties of this nature were encountered.

Sorption Isotherm. Figure 5 shows the sorption isotherm for PS/ethylbenzene at 40 °C prepared from the apparent equilibrium uptakes in Figure 3. The apparent equilibrium weight fraction is plotted against the ratio of the manifold pressure, p_1, to the vapor pressure of ethylbenzene at 40 °C, p_1°, calculated from Antoine's equation.[27] Figure 5 also shows two predictions from the Flory–Huggins solution theory,[28] which gives the following expression for p_1/p_1° as a function of composition in the limit that M_2 is very large:

$$p_1/p_1^\circ = v_1 \exp(v_2 + \chi v_2^2) \tag{7}$$

where χ is the Flory–Huggins interaction parameter and v_i is the volume fraction of component i, related to the weight fraction by

$$v_i = \frac{\omega_i \hat{V}_i}{\omega_1 \hat{V}_1 + \omega_2 \hat{V}_2} \tag{8}$$

Here, $\hat{V}_i$ means the partial specific volume of component i. These were taken as the specific volumes of pure ethylbenzene and PS[29,30] in preparing Figure 5, which neglects the very small volume change on mixing in this system.[30]

Our data are fit best with $\chi = 0.05$, consistent with ethylbenzene being a good solvent for PS.[32] Duda et al.[31] found that $\chi = 0.45$ gave a good fit to sorption isotherms in this system at temperatures well above 100 °C; this value does not describe our data (see Figure 5). The discrepancy cannot be accounted for by the difference in temperature, since χ typically decreases with temperature, but could be due to differences in polymer molecular weight, molecular weight distribution, solvent purity, or as is most likely, the inaccuracy of our pressure readings (see below).

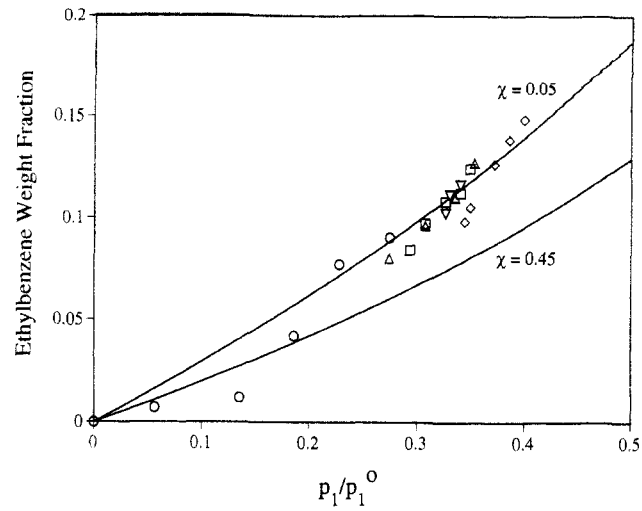

Figure 5. Sorption isotherm for poly(styrene)/ethylbenzene at 40 °C based on equilibrium uptakes from pass 1 (○), pass 2 (△), pass 3 (□), pass 4 (▽), and pass 5 (◇) along with the predictions of the Flory–Huggins expression for $\chi = 0.45$ and $\chi = 0.05$.

The reader should note that we ignored two data points at the lowest ethylbenzene pressures when fitting eq 7 to the data because we had less confidence in the measured equilibrium uptakes for these runs: The sorption process was extremely long for these conditions, and it is likely that the true equilibrium uptake was not achieved. This suspicion is reinforced by the fact that at the lowest values of ethylbenzene concentration, the data fall well below the fit to the remaining points. The relatively larger scatter of the remaining data is due to the rather crude method we used of measuring the pressure in the manifold. A mercury manometer of limited accuracy was used (p_1 could only be read to within ±0.1 Torr). As a result, the relative error in p_1/p_1° is not better than ±10–20%.

Reproducibility of Dynamic Data. Many years ago it was observed that the time scale for integral sorption progressively increased with successive sorption–desorption cycles in the systems cellulose nitrate/acetone[33] and poly(styrene)/benzene.[34] In both cases, the change in sorption behavior was accompanied by a significant increase in orientation of the polymer chains along the direction of diffusion, presumably induced by the repeated, unidirectional swelling of the film. So, an initial concern with the use of multiple passes in our work was that each pass might cause some progressive structural change which could affect the diffusion process. To check this, we examined the reproducibility of sorption data collected in separate passes at roughly the same mean ethylbenzene weight fraction, $\langle\omega_1\rangle$.

Figure 6a shows the relative weight uptake, M_t/M_∞, plotted against $\sqrt{t}$ for runs R5 ($\langle\omega_1\rangle = 0.0837$) and R6 ($\langle\omega_1\rangle = 0.0878$); both uptake curves are the two-stage type. The data for the two runs coincide quite well over the entire time scale. Figure 6b shows a comparison of M_t/M_∞ versus $\sqrt{t}$ for runs R7 ($\langle\omega_1\rangle = 0.1026$), R10 ($\langle\omega_1\rangle = 0.1023$), and R15 ($\langle\omega_1\rangle = 0.1017$), which are all the sigmoid type. The data for all three runs are consistent over the whole time scale. Figure 6c shows the reproducibility for the Fickian process, which was found at the highest ethylbenzene contents. The plot shows M_t/M_∞ versus $\sqrt{t}$ for runs R8 ($\langle\omega_1\rangle = 0.1185$) and R12 ($\langle\omega_1\rangle = 0.1181$). Although data at short times are absent in R8, as equilibrium uptake is approached, the two data sets show excellent agreement.

Figure 6d shows a similar plot for runs R11 ($\langle\omega_1\rangle = 0.1101$), R14 ($\langle\omega_1\rangle = 0.1138$), and R16 ($\langle\omega_1\rangle = 0.1156$). All three curves are the sigmoid type as in Figure 6b, but $\langle\omega_1\rangle$

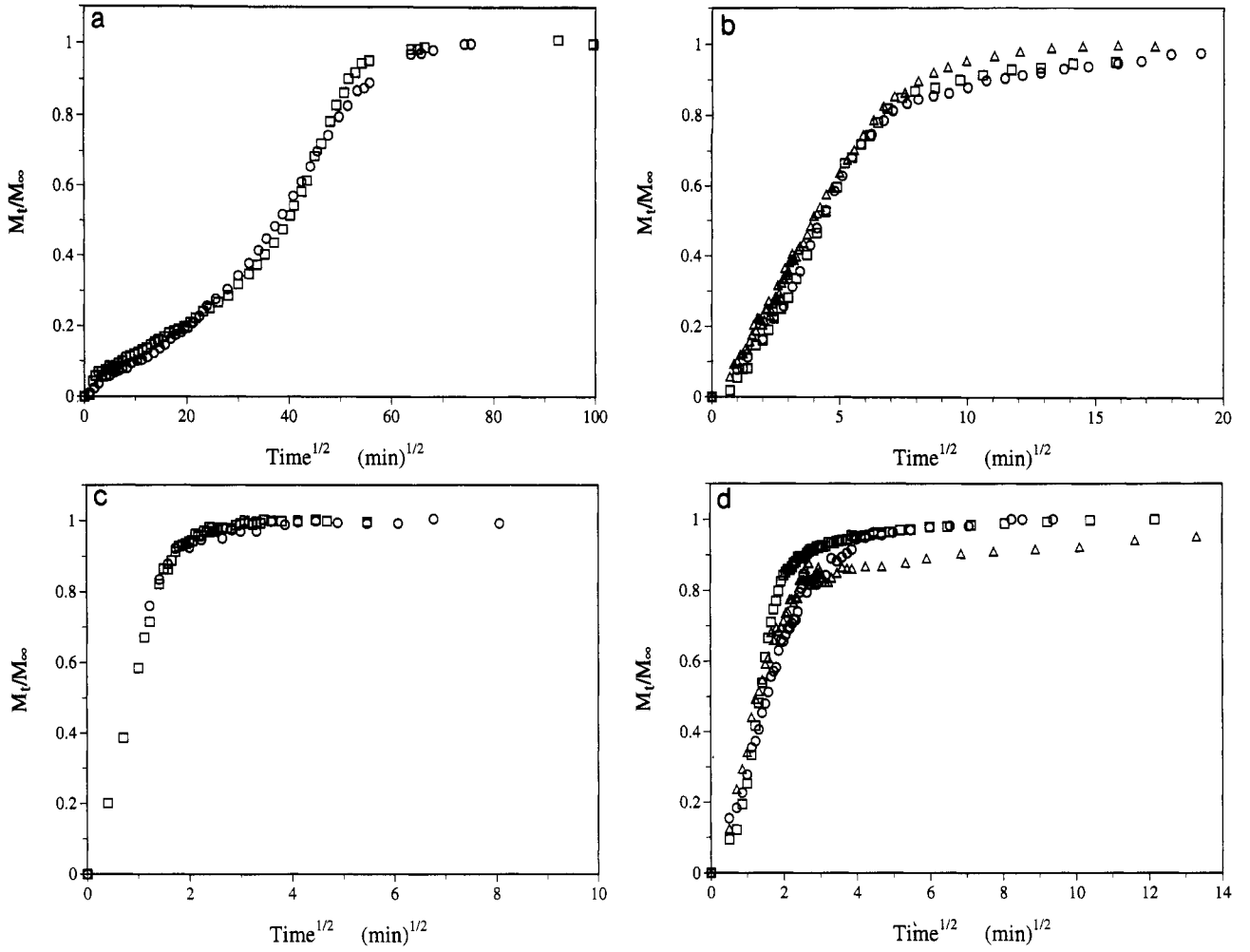

Figure 6. (a) M_t/M_∞ versus $\sqrt{t}$ for runs R5 (○) ($\langle\omega_1\rangle$ = 0.0837) and R6 (□) ($\langle\omega_1\rangle$ = 0.0878) demonstrating reproducibility. (b) M_t/M_∞ versus $\sqrt{t}$ for runs R7 (○) ($\langle\omega_1\rangle$ = 0.1026), R10 (□) ($\langle\omega_1\rangle$ = 0.1023), and R15 (△) ($\langle\omega_1\rangle$ = 0.1017) demonstrating reproducibility. (c) M_t/M_∞ versus $\sqrt{t}$ for runs R8 (○) ($\langle\omega_1\rangle$ = 0.1185) and R12 (□) ($\langle\omega_1\rangle$ = 0.1181) demonstrating reproducibility. (d) M_t/M_∞ versus $\sqrt{t}$ for runs R11 (○) ($\langle\omega_1\rangle$ = 0.1101), R14 (△) ($\langle\omega_1\rangle$ = 0.1138), and R16 (□) ($\langle\omega_1\rangle$ = 0.1156) demonstrating reproducibility.

and $\Delta\omega_1$ vary more significantly than among the runs shown in Figure 6b. At short times, agreement between the data sets is satisfactory, but as equilibrium is approached, the curves diverge significantly. Run R16, in particular, which has the largest $\langle\omega_1\rangle$ among the runs appearing in Figure 6d, approaches equilibrium more quickly than do the others.

From these comparisons, it should be clear that the sorption data are, in fact, very reproducible in the range $0.08 < \langle\omega_1\rangle < 0.12$. This demonstrates that the use of multiple passes did not induce progressive structural change in the polymer.

Trends in Dynamic Behavior with Composition. We now discuss in detail the trends evident in the sorption kinetics as $\langle\omega_1\rangle$ is increased. Figure 7a shows the behavior for the lowest ethylbenzene contents. The relative weight uptake, M_t/M_∞ is plotted against $\sqrt{t}$ for runs R1 ($\langle\omega_1\rangle$ = 0.0036) and R2 ($\langle\omega_1\rangle$ = 0.0099) with the data for the latter run shifted as in Figure 4. Except for a short apparent induction time in R1, the two data sets essentially coincide, indicating a lack of concentration dependence in the transport properties over the small concentration range spanned by the two intervals. In both runs, the weight uptake proceeds in a slow monotonic fashion consistent with the behavior termed pseudo-Fickian in sequence 1. Two features of concern in these runs are their low apparent equilibrium uptake (see Figure 5) and their short time scale relative to run R3 (see Figure 3a). Both features suggest that we have not tracked the sorption process long enough to achieve a true equilibrium.

At higher ethylbenzene contents, the sorption behavior is clearly two-stage. Figure 7b shows M_t/M_∞ versus $\sqrt{t}$ for runs R3 ($\langle\omega_1\rangle$ = 0.0276), R4 ($\langle\omega_1\rangle$ = 0.0600), and R5 ($\langle\omega_1\rangle$ = 0.0837). The initial, diffusion controlled stages for all three runs are essentially coincident. These account for only ~10–15% of the total fluid uptake in each run. The second, relaxation controlled stages, which account for the majority of the uptake, are shifted to shorter time scales with increasing fluid content. At still higher ethylbenzene contents, the fluid weight uptake curves change progressively from two-stage to sigmoid. Figure 7c shows M_t/M_∞ versus $\sqrt{t}$ for runs R5 ($\langle\omega_1\rangle$ = 0.0837), R9 ($\langle\omega_1\rangle$ = 0.0.0905), and R7 ($\langle\omega_1\rangle$ = 0.1026). As in Figure 7b, increasing $\langle\omega_1\rangle$ causes the second stage to shift to shorter time scales; this continues until in run R7, the initial stage of the two-stage uptake is no longer clearly discernible and the weight uptake curve appears S-shaped or sigmoid initially.

We observed a *very* sudden change with $\langle\omega_1\rangle$ in the time scale for sorption just beyond run R9 (see Table I). We associate this with the point where the glass transition temperature of the polymer–fluid mixture gets depressed to the experimental temperature. In particular, the observation suggests that T_g of a PS/ethylbenzene mixture should correspond to ≃40 °C at an ethylbenzene content just beyond that for run R9, i.e. for $\langle\omega_1\rangle$ somewhat greater than 0.0905. This is supported by measurements of T_g in PS/ethylbenzene mixtures. Figure 8 shows a plot of the change in T_g from the dry polymer's value, ΔT_g, versus fluid weight fraction, ω_1, based on the dilatometric data

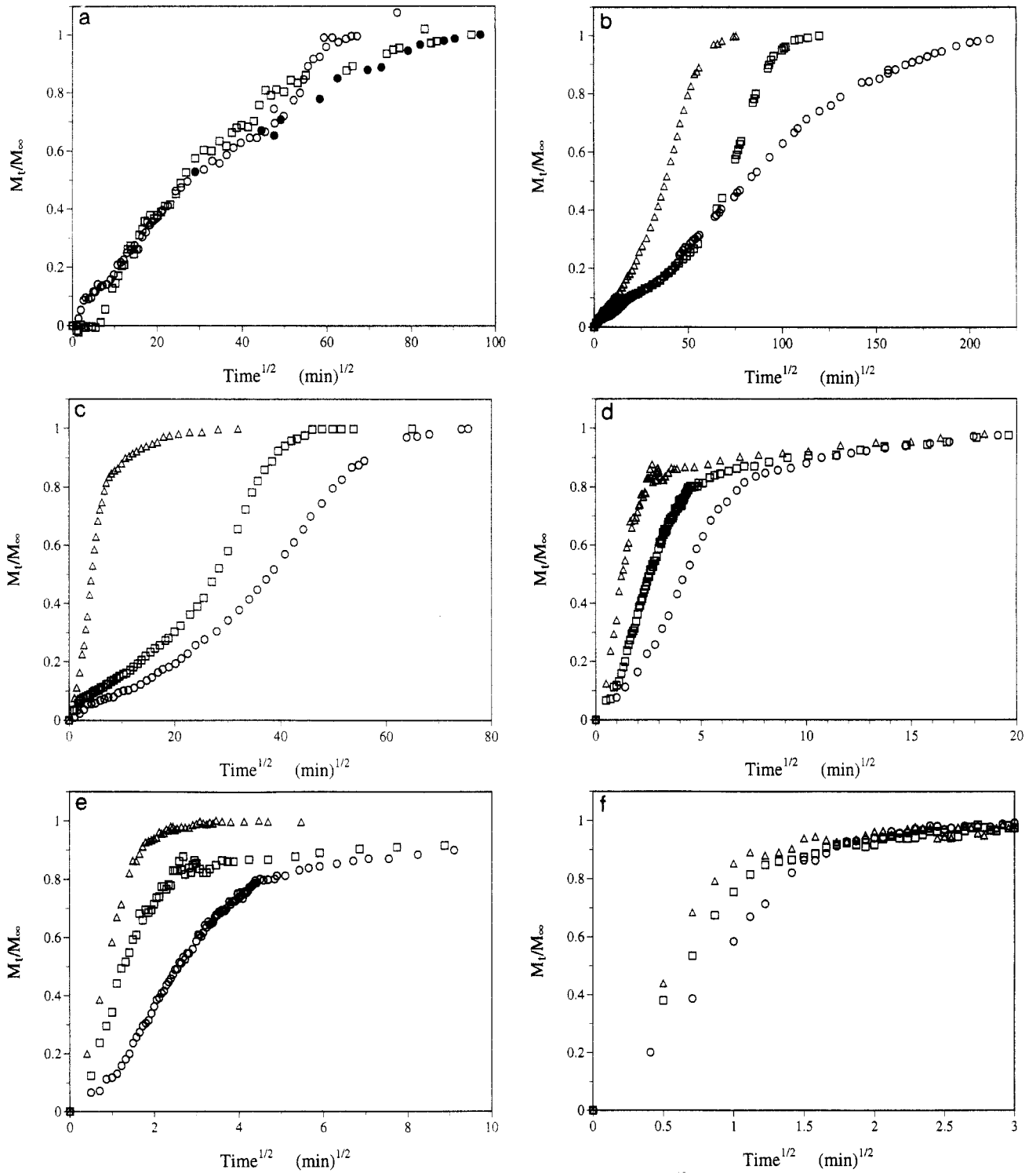

Figure 7. (a) M_t/M_∞ versus $\sqrt{t}$ for runs R1 (□) ($\langle\omega_1\rangle$ = 0.0036) and R2 (○, ●) ($\langle\omega\rangle$ = 0.0099) illustrating trend in sorption kinetics with $\langle\omega_1\rangle$. (b) M_t/M_∞ versus $\sqrt{t}$ for runs R3 (○) ($\langle\omega_1\rangle$ = 0.0276), R4 (□) ($\langle\omega_1\rangle$ = 0.0600), and R5 (△) ($\langle\omega_1\rangle$ = 0.0837) illustrating trend in sorption kinetics with $\langle\omega_1\rangle$. (c) M_t/M_∞ versus $\sqrt{t}$ for runs R5 (○) ($\langle\omega_1\rangle$ = 0.0837), R9 (□) ($\langle\omega_1\rangle$ = 0.0905), and R7 (△) ($\langle\omega_1\rangle$ = 0.1026) illustrating trend in sorption kinetics with $\langle\omega_1\rangle$. (d) M_t/M_∞ versus $\sqrt{t}$ for runs R7 (○) ($\langle\omega_1\rangle$ = 0.1026), R13 (□) ($\langle\omega_1\rangle$ = 0.1068), and R14 (△) ($\langle\omega_1\rangle$ = 0.1138) illustrating trend in sorption kinetics with $\langle\omega_1\rangle$. (e) M_t/M_∞ versus $\sqrt{t}$ for runs R13 (○) ($\langle\omega_1$ = 0.1068), R14 (□) ($\langle\omega_1\rangle$ = 0.1138), and R12 (△) ($\langle\omega_1\rangle$ = 0.1181) illustrating trend in sorption kinetics with $\langle\omega_1\rangle$. (f) M_t/M_∞ versus $\sqrt{t}$ for runs R12 (○) ($\langle\omega_1\rangle$ = 0.1181), R17 (□ ($\langle\omega_1\rangle$ = 0.1308), and R18 (△) ($\langle\omega_1\rangle$ = 0.1425) illustrating trend in sorption kinetics with $\langle\omega_1\rangle$.

Table I. Square Root of Half-Time for Sorption, $t^{*1/2}$

run	$\langle\omega_1\rangle$	$t^{*1/2}$ (min$^{1/2}$)
R3	0.0276	81.4
R4	0.0600	71.1
R5	0.0837	38.0
R9	0.0905	27.7
R7	0.1026	4.3
R13	0.1068	2.6
R14	0.1138	1.3

of Ueberreiter.[35] The plot indicates a linear relationship between ΔT_g and ω_1 in the concentrated polymer limit. Now, the mean ethylbenzene weight fraction for run R9, where the drastic time scale change for sorption occurred, is $\langle\omega_1\rangle$ = 0.0905; for this composition, Ueberreiter's data imply a glass transition temperature of 41.4 °C, which is just above the experimental temperature in this study.

At ethylbenzene contents higher than that for run R9, sigmoid weight uptake curves are found which continue to shift to shorter time scales with increasing ethylbenzene content. Figure 7d illustrates this with plots of M_t/M_∞ versus $\sqrt{t}$ for runs R7 ($\langle\omega_1\rangle$ = 0.1026), R13 ($\langle\omega_1\rangle$ = 0.1068),

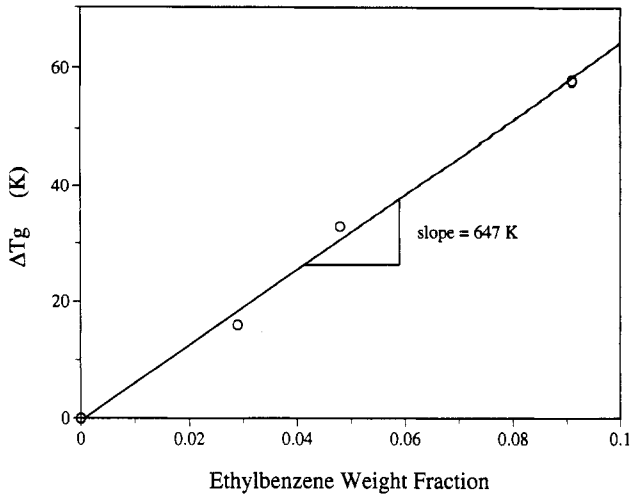

Figure 8. ΔT_g versus ω_1 for poly(styrene)/ethylbenzene mixtures. The solid line is a linear regression fit. (Based on the dilatometric data in ref 35).

and R14 ($\langle\omega_1\rangle = 0.1138$). Careful inspection of these data reveals an interesting feature in all three uptake curves: Above $M_t/M_\infty \simeq 0.8$, the approach to equilibrium is very gradual, in fact, too gradual for ordinary diffusion. The process resembles the second stage of a two-stage weight uptake curve in the case that the second stage makes a very small contribution to the total weight uptake. Although this feature is unmistakable, discerning trends in it with $\langle\omega_1\rangle$ is difficult due to the protracted nature of the process and the small weight changes involved.

As the ethylbenzene content is increased further, the weight uptake curves change from sigmoid to Fickian. Figure 7e shows a plot of M_t/M_∞ versus $\sqrt{t}$ for runs R13 ($\langle\omega_1\rangle = 0.1068$), R14 ($\langle\omega_1\rangle = 0.1138$), and R12 ($\langle\omega_1\rangle = 0.1181$). In run R12, the weight uptake plot is linear with $\sqrt{t}$; the initial, sigmoid shape and the gradual, secondary relaxation to equilibrium which are clear in runs R13 and R14 have disappeared. Figure 7f shows M_t/M_∞ versus $\sqrt{t}$ for runs R12 ($\langle\omega_1\rangle = 0.1181$), R17 ($\langle\omega_1\rangle = 0.1308$), and R18 ($\langle\omega_1\rangle = 0.1425$) which are all clearly Fickian. For these uptake curves, the initial slope, and therefore the polymer material diffusion coefficient, increase with increasing ethylbenzene content.

Differential sorption experiments at even higher ethylbenzene contents were not undertaken for three reasons. First, it was increasingly difficult to supply ethylbenzene vapor to the manifold at pressures above the room temperature equilibrium vapor pressure ($\simeq$7.1 Torr). Secondly, by run R18 the polymer film was well above its glass transition and there was noticeable evidence of flow near the top of the film sample. Thirdly, by run R18 the kinetics of the sorption process were too fast to follow accurately in our equipment.

Summary and Conclusions

We designed and constructed a quartz-spring vapor sorption balance permitting the study of linear viscoelastic mutual diffusion in the poly(styrene)/ethylbenzene system via the differential sorption technique. The design criteria for the equipment, and for the experimental program, were based on the Deborah number correlation of Vrentas and Duda[20,21] which purports to predict the conditions where linear viscoelastic diffusion should be clearly observed in a polymeric/simple-fluid mixture.

The experimental program consisted of 18 differential sorptions on a thin film (5.0 μm) of nearly monodisperse poly(styrene) ($\bar{M}_n = 305\,000$, $\bar{M}_w/\bar{M}_n = 1.05$) at 40 °C using the smallest possible increments in ethylbenzene pressure. Using small pressure increments ($\sim$1 Torr) is essential for linear diffusion experiments because of the extreme sensitivity of the transport properties to composition in this system.[31]

The data were collected in five separate passes, each beginning at a low ethylbenzene pressure and terminating at a higher ethylbenzene pressure after a number of successive differential sorptions. Sorption runs from different passes, but at the same mean ethylbenzene weight fraction $\langle\omega_1\rangle$, showed good agreement in all cases, indicating that no progressive structural changes took place during the experiments (e.g. aging or orientation).

The sorption isotherm from the equilibrium uptake at each ethylbenzene pressure was fit with the Flory–Huggins expression using an interaction parameter $\chi = 0.05$. This value lies below that expected from previous work;[31] the discrepancy is likely due to the relatively inaccurate method used for measuring pressure in the apparatus.

The kinetic sorption data showed systematic changes with increasing ethylbenzene weight fraction, $\langle\omega_1\rangle$. The weight uptake curves in the range $0.0276 < \langle\omega_1\rangle < 0.1138$ were clearly viscoelastic (non-Fickian). Two distinct viscoelastic responses were seen in this range: two-stage weight uptake and sigmoid weight uptake with a protracted approach to equilibrium. The weight uptake curves for $\langle\omega_1\rangle > 0.1138$ appeared to be Fickian. The uptake curves for $\langle\omega_1\rangle < 0.0276$ appear to correspond to the pseudo-Fickian process in sequence 1; however the data are not of the best quality: The sorptions were difficult to follow because of the extremely long time scale and one run at these conditions suffered from a mishap.

The data clearly show that viscoelastic diffusion is encountered over a broader range of ethylbenzene weight fractions than anticipated by the $(DEB)_D$ calculation outlined by Vrentas and Duda;[21] the correlation (Figure 2) predicts that viscoelastic diffusion should be seen in the range $0.07 < \langle\omega_1\rangle < 0.12$, while the data show viscoelastic effects at weight fractions as low as $\langle\omega_1\rangle \simeq 0.03$. That viscoelastic diffusion is seen at lower concentrations than anticipated by eq 6 suggests that relaxation processes with time scales shorter than the terminal time τ are involved in viscoelastic diffusion for relatively low values of $\langle\omega_1\rangle$. In particular, relaxation mechanisms associated with the transition region of the linear viscoelastic spectrum appear to play an important role in viscoelastic diffusion at these conditions. By this line of thought, the fact that viscoelastic effects persist up to $\langle\omega_1\rangle = 0.1138$, in reasonable agreement with the upper bound anticipated from Figure 2, suggests that the mechanisms associated with the terminal time become involved, and perhaps play the dominant role, for viscoelastic diffusion at relatively high values of $\langle\omega_1\rangle$.

The data reveal the following characteristic sequence of sorption behaviors with increasing $\langle\omega_1\rangle$:

pseudo-Fickian → two-stage → pseudo-sigmoid → Fickian (9)

where pseudo-sigmoid refers to an uptake curve which is initially S-shaped, but with a protracted approach to equilibrium. Except for the pseudo-Fickian curves at the lowest ethylbenzene contents, where we suspect we have not waited long enough for the true equilibrium, the time scale needed to achieve equilibrium consistently decreased with increasing ethylbenzene content. We observed a very sudden decrease in the sorption time scale at the transition from two-stage to pseudo-sigmoid behavior. The composition where this occurred, $\langle\omega_1\rangle \simeq 0.095$, is where T_g of the mixture is depressed to the experimental temperature. This is supported by the dilatometric data of Uberreiter[35] on poly(styrene)/ethylbenzene mixtures.

The sequence 9 is similar to that found by Odani et al.[8-11] (sequence 1). The two sequences show two main differences: (1) sequence 9 does not exhibit sigmoid uptake curves at the lowest fluid concentrations, as in sequence 1, but rather shows pseudo-Fickian and two-stage uptake, (2) sequence 9 reveals at relatively high fluid contents a transition from two-stage to Fickian uptake via pseudo-sigmoid uptake curves, rather than via pseudo-Fickian uptake curves, as in sequence 1.

These differences are probably due to a combination of two factors. First, we believe that our data are more accurate than those reported in refs 8–11, since our springs and cathetometer are more sensitive by about 1 order of magnitude than the corresponding equipment described in the Japanese study. We also recorded a much higher density of data points than in the previous work. Consequently, the fine details in the weight uptake plots could have been missed by the earlier investigators. For example, at the low fluid contents, sigmoid uptakes were reported. These might actually have been two-stage plots in which the first stage has a small enough uptake to make the relatively imprecise data appear as a sigmoid. So, the true nature of the uptake plots could well be the same in both studies.

Along the same line of thought, consider the pseudo-sigmoid uptakes in sequence 9 which show mild upward curvature initially, followed by a slow approach to equilibrium (see Figure 7d, for example). With less accurate equipment and fewer data points, the initial upward curvature could be missed with the result that only the protracted approach to equilibrium is noticed; such behavior would naturally be described as pseudo-Fickian.

A second factor probably contributing to the difference between sequences 1 and 9 is the difference in polymer molecular weight distributions: our sample is nearly monodisperse while those used in the Japanese work had broad distributions. Consequently, the samples studied by Odani et al. probably possessed a much broader, less-structured distribution of relaxation times contributing to viscoelastic effects and, therefore, a somewhat different sequence of viscoelastic sorption curves could have occurred.

Acknowledgment. This work was supported by the National Science Foundation (Grants CBT-86-17369 and CTS-89-19665).

References and Notes

(1) Fujita, H. *Fortsch. Hoch. Polym. Forsch.* **1964**, *3*, 1.
(2) Vrentas, J. S.; Duda, J. L. In *Encyclopedia of Polymer Science and Engineering*; Bikales, N., Kroschewitz, J., Eds.; John Wiley: New York, 1986.
(3) Durning, C. J.; Tabor, M. *Macromolecules* **1986**, *19*, 2220.
(4) Durning, C. J. *J. Polym. Sci., Polym. Phys. Ed.* **1985**, *23*, 1831.
(5) Mehdizahdeh, S.; Durning, C. J. *AIChE J.* **1990**, *36*, 877.
(6) Billovits, G. F.; Durning, C. J. *Polym. Commun.* **1990**, *31*, 358.
(7) Lustig, S. R.; Caruthers, J. M.; Peppas, N. *Chem. Eng. Sci.* **1992**, *47*, 3037.
(8) Kishimoto, A.; Fujita, H.; Odani, H.; Kurata, M.; Tamura, M. *J. Phys. Chem.* **1960**, *64*, 594.
(9) Odani, H.; Kida, S.; Kurata, M.; Tamura, M. *Bull. Chem. Soc. Jpn.* **1961**, *34*, 571.
(10) Odani, H.; Hayashi, J.; Tamura, M. *Bull. Chem. Soc. Jpn.* **1961**, *34*, 817.
(11) Odani, H.; Kida, S.; Tamura, M. *Bull. Chem. Soc. Jpn.* **1966**, *39*, 2378.
(12) Richards, W. D.; Prud'homme, R. K. *J. Appl. Polym. Sci.* **1986**, *31*, 763.
(13) Crank, J.; Park, G. S. in *Diffusion in Polymers*; Crank, J., Park, G. S., Eds.; Academic Press: London, 1968.
(14) (a) Hwang, D.; Cohen, C. *Macromolecules* **1984**, *17*, 1679. (b) Hwang, D.; Cohen, C. *Macromolecules* **1984**, *17*, 2890.
(15) Lasky, R. C.; Kramer, E.; Hui, C. Y. *Polymer* **1988**, *29*, 673.
(16) Tong, H. M.; Saenger, K.; Durning, C. J. *J. Polym. Sci., Polym. Phys. Ed.* **1989**, *27*, 689.
(17) Berens, A. R.; Hopfenberg, H. B. *Polymer* **1978**, *19*, 489.
(18) Vrentas, J. S.; Duda, J. L.; Hou, A. C. *J. Appl. Polym. Sci.* **1984**, *29*, 399.
(19) Vrentas, J. S.; Duda, J. L.; Huang, W. J. *Macromolecules* **1986**, *19*, 1718.
(20) Vrentas, J. S.; Jarzebski, C. M.; Duda, J. L. *AIChE J.* **1975**, *21*, 94.
(21) Vrentas, J. S.; Duda, J. L. *J. Polym. Sci., Polym. Phys. Ed.* **1977**, *15*, 441.
(22) Vrentas, J. S.; Duda, J. L. *J. Polym. Sci., Polym. Phys. Ed.* **1977**, *15*, 403.
(23) Vrentas, J. S.; Duda, J. L. *J. Polym. Sci., Polym. Phys. Ed.* **1977**, *15*, 417.
(24) Bueche, F. *Physical Properties of Polymers*; Interscience: New York, 1962.
(25) Fujita, H.; Kishimoto, A. *J. Polym. Sci.* **1958**, *28*, 547.
(26) Prager, S.; Long, F. A. *J. Am. Chem. Soc.* **1951**, *73*, 4072.
(27) Dean, J. A. *Lange's Handbook of Chemistry*, 12th ed.; McGraw Hill: New York, 1979.
(28) Flory, P. J. *Principles of Polymer Chemistry*; Cornell University Press: Ithaca, New York, 1953.
(29) Barlow, A. J.; Lamb, J.; Matheson, A. J. *Proc. R. Soc.* **1966**, *A292*, 322.
(30) Hocker, H.; Blake, G. J.; Flory, P. J. *Trans. Faraday Soc.* **1971**, *67*, 2270.
(31) Duda, J. L.; Vrentas, J. S.; Ju, S. T.; Liu, H. T. *AIChE J.* **1982**, *28*, 279.
(32) Brandrup, J.; Immergut, E. H. *Polymer Handbook*, 2nd ed.; John Wiley: New York, 1975.
(33) Drechsel, P.; Hoard, J. L.; Long, F. A. *J. Polym. Sci.* **1953**, *10*, 241.
(34) Long, F. A.; Kokes, R. J. *J. Am. Chem. Soc.* **1953**, *75*, 2232.
(35) Ueberreiter, K. *Angew. Chem.* **1940**, *53*, 247.